ENGSCI 700A/B
Department of Engineering Science

Project 41: Make Womb

An investigation of vascular Adaptation to Pregnancy

Final Report

Jungwoo Han

UPI: jhan603

Student ID: 512163833

Abstract

For a developing fetus to grow healthily, the mother must provide enough oxygen and nutrient-rich blood to the surface of the placenta via the uterus. As the fetus continues to develop and grow, it demands more oxygen and nutrients, which leads to a significant increase in the blood flow required in the uterus during pregnancy. In the uterus, volumetric blood flow increases by 15-fold across the nine months of pregnancy. To meet the requirements the fetus requires, the blood vessels increase dramatically in size in response to interacting impacts of hormonal influences and vessel haemodynamics. The process of understanding the mechanisms involved in this process will need a thorough understanding and failure to accommodate this flow has a significant impact on the baby's health. To understand how the arteries in the uterus respond to both blood flow and hormones typical of pregnancy. This project aims to understand how the uterine arteries change in pregnancy; our approach is in two aligned areas: using image analysis techniques to understand how the uterine arteries change in early pregnancy and using computational modeling to relate structure to function in the uterine blood vessels.

Contents

1 Notations **3**

2 Acknowledgements **4**

3 Literature Review **5**
- 3.1 Motivation . . . 5
- 3.2 Fetal Growth Restriction . . . 5
- 3.3 Hormonal Influences . . . 5
- 3.4 The Uterus . . . 6
- 3.5 The Placenta . . . 6
- 3.6 Changes In Uterine Circulation . . . 7
- 3.7 Spiral Arteries Remodelling . . . 8
- 3.8 Arcuate and Radial artery remodelling . . . 9
- 3.9 Medical Imaging Analysis on Boyd Collection . . . 9
- 3.10 ImageJ Image Analysis on Placental Histological sections . . . 10
- 3.11 Deep Placental Vessel Segmentation in Fetoscopic Images . . . 11

4 Methods **12**
- 4.1 Data Collection . . . 12
- 4.2 Setting up the Environment . . . 13
- 4.3 Filtering out Images . . . 15
- 4.4 Splitting to Sub-Images . . . 15
- 4.5 Decoding to Tensors . . . 16
- 4.6 Verify Corresponding Pairs and Removing Unnecessary Images . . . 16
- 4.7 Choice of Machine Learning Models and Tasks . . . 17
- 4.8 Development of Model . . . 17
  - 4.8.1 Format of Input Data . . . 17
  - 4.8.2 Models Training and Optimization . . . 18
- 4.9 Predictions Visualization . . . 19
- 4.10 Python Image Analysis . . . 19

5 Results and Discussion **20**
- 5.1 Machine Learning Model Results . . . 20
- 5.2 Python Image Analysis Results . . . 21
- 5.3 Combining the Results . . . 22

6 Conclusion **23**

References **24**

1 Notations

- FGR - Fetal Growth Restriction
- hcG - human chorionic gonadtropin
- CNN - Convolutional Neural Network
- ML - Machine Learning

2 Acknowledgements

First and foremost, I extend the deepest gratitude to the supervisor, Alys Clark, for their unwavering guidance, support and expertise throughout this research project. Their valuable insights and mentorship have been instrumental in shaping the direction of this research.

I am also thankful to the members of the Auckland Bio-engineering Institute, especially Jo James, for their constructive feedback and expertise that made me have a better understanding of the biology aspect related to this project.

I would like to express the sincere gratitude and appreciation to Savindi Wijenayaka. Despite our brief interaction, her invaluable assistance in resolving coding issues was instrumental in the successful completion of the project. Her guidance and support were truly indispensable during a critical phase of the project.

Finally I would like to give thanks to the project partner Daniel.

I would finally like to thank the friends and family who have been supporting me and encouraging me throughout the year while I faced many challenges when working on this project.

3 Literature Review

3.1 Motivation

FGR presents a significant challenge in maternal and fetal health, and it is a condition of pregnancy where the fetus does not grow as large as it should. While FGR is clinically detectable in the later stages of pregnancy, the underlying factors often initiate much earlier. The uterine arteries, mainly the uterine, arcuate, and radial arteries, play a pivotal role in blood flow to the placenta. This literature review explores existing knowledge and research on uterine arterial remodeling during pregnancy. The aim is to investigate how the uterine arteries respond to increased blood flow and pregnancy-related hormones, specifically focusing on early pregnancy. This review will also examine image analysis and machine learning techniques for identifying structural changes in placental tissue.

3.2 Fetal Growth Restriction

FGR is a condition that affects roughly 5 to 10% of pregnancies (S. Medicine, n.d.) and is a leading cause of perinatal mortality and is responsible for 30% of stillborn infants. Currently, there are no treatments to control FGR, so it must be detected early so it can be monitored carefully and help minimize risks. A factor that FGR exhibits is a change in the site of placental implantation, and this is when the placenta attaches itself to the upper part of the uterus, which allows an optimal environment for it to provide nutrients and oxygen to the fetus. When there is an abnormal placental implantation, if it attaches to a different area of the uterus, it can lead to increased resistance in the uterine artery (Nardozza et al., 2017).

3.3 Hormonal Influences

During pregnancy, the hormone levels of a woman will change to accompany pregnancy. Hormones such as oestrogen, testosterone, and progesterone can fluctuate to provide different kinds of support throughout particular stages of pregnancy. Oestrogen and progesterone are produced in early pregnancy to support the baby until the placenta takes over. These hormones help the development of the fetus's organs and the correct function of the placenta (NCT, 2018).

Another crucial hormone is human chorionic gonadotropin (hcG). It is called the pregnancy hormone because it is only produced during pregnancy. It functions by telling the body to create more estrogen and progesterone. Together with hCG, these hormones help thicken the uterine lining and help the body to stop menstruating. The correct balance of these three hormones sustains and supports the pregnancy (Clinic, 2022).

These hormones are derived from the placental environment to help relax and smooth the muscle that forms the walls of the arteries, and this is a response to the change in levels of hormones. Another change that occurs due to the change in hormone levels is a change in haemodynamics. The main important change is the gradual increase in blood volume over gestation, reaching a 40% increase by term but with great individual variability. Red blood

cells increase their mass by 30%, and the arteries increase in blood flow and production rate of red blood cells (Thornburg, Jacobson, Giraud, & Morton, 2000). Combining these different changes causes the muscles to relax, increasing cardiac output. The placenta wants to supply oxygen to the fetus, which needs consistent oxygen. There are consequences when there is an inconsistent oxygen supply to the fetus. These consequences are possible diseases that arise from the intermittent supply of oxygen.

This leads to another cause of FGR, which is a reduced blood flow from the placenta to the uterus, so less oxygen and nutrients are being delivered to the fetus, as the fetus relies on placental perfusion for adequate oxygenation and nutrient supply. When blood flow is compromised, the circulatory and metabolic demands of the fetus may not be met, and FGR can result (Morley, Debant, Walker, Beech, & Simpson, 2021).

A common health issue that affects fetal growth is the most common nutritional disorder, iron deficiency anemia. During the third trimester, fetal iron demands rise, concurrent with increased fetal growth. If maternal iron deficiency anemia is present during the early third trimester, it could potentially lead to fetal growth restriction due to insufficient circulation and tissue oxygenation (Madendag et al., 2019).

3.4 The Uterus

The uterus is a thick-walled muscular structure that lies in the midline of the abdominal pelvic cavity and plays a crucial role in the reproductive system. There are a few processes that the uterus is responsible for, and they are implantation, gestation, menstruation, and labor. The process interested is the gestation process, where the uterus serves as an environment for the fetus to grow during pregnancy while also providing it with oxygen and nutrients through the placenta by supplying nutrient-rich blood to the surface of the placenta. The uterus consists of 3 layers: the endometrium (innermost layer), myometrium, and the perimetrium (outermost layer) (Gasner & P A, 2023). The three different layers serve different purposes in the reproductive process. The endometrium lines the uterine cavity, and if no egg is implanted, it is shed during menstruation. The myometrium comprises smooth muscle fibers, and the perimetrium is a thin layer of connective tissue covering the uterus (Ameer, Fagan, Sosa-Stanley, & Peterson, 2022).

3.5 The Placenta

The placenta is a temporary organ that develops in the uterus during pregnancy. It supports the growth and development of the fetus during pregnancy. The main functions of the placenta can be categorized as transportation and protection. The placenta provides oxygen, water, vitamins, and other essential nutrients for the growth of the fetus while also removing carbon dioxide and other waste products from the bloodstream that could be toxic to the mother and the fetus. Other functions it provides are releasing hormones that allow for a suitable environment for fetal growth (Gude, Roberts, Kalionis, & King, 2004). These hormones, as mentioned previously, are oestrogen, progesterone, and human chorionic gonadotropin (hCG). Oestrogen, produced by the ovaries and later the placenta, promotes

uterine and placental growth, ensuring the development of fetal organs, and increases blood flow to the uterus, which supplies nutrients and oxygen to the growing fetus. Progesterone, also produced by the ovaries and placenta, plays a crucial role in maintaining the uterine environment, preventing premature contractions, and ensuring a thick uterine lining to support the embryo. Meanwhile, hCG, known as the pregnancy hormone, prevents menstruation and signals the body to continue producing estrogen and progesterone, safeguarding the pregnancy.

Gross anatomical changes in the FGR placenta include a smaller placental diameter and chorionic plate area. This reduction limits the number of spiral arteries that trophoblasts can remodel, affecting perfusion and nutrient exchange. 3D ultrasounds have shown that fetuses destined for FGR exhibit decreased placental volume in the first trimester due to reductions in both diameter and thickness (Sun et al., 2020).

3.6 Changes In Uterine Circulation

Utero-placental is the blood flow between the mother's uterus and the placenta. Where the maternal blood enters the placenta through spiral arteries traversing into the intervillous spaces and flows around the villi, where the maternal blood can exchange nutrients and oxygen with fetal blood and drains back into the placenta (Sapehia et al., 2021).

The major uterine blood vessels in the uterus consist of uterine arteries and veins and spiral, radial, and arcuate arteries. Uterine arteries provide oxygenated blood to the uterus, with branches supplying the uterine walls and cervix, and also control the amount of blood that gets to the placenta (Allerkamp, Pole, Boukham, James, & Clark, 2022). Spiral arteries within the endometrium play a crucial role during pregnancy by delivering nutrients and oxygen to the placenta, ensuring fetal nourishment. Arcuate arteries support the outer myometrial layer. For a visual representation of the different arteries in a pregnant and non-pregnant uterus, refer to Figure 1 below.

During pregnancy, two major adaptations occur, firstly the spiral arteries are remodeled from being tightly coiled to wide tubes that lack responsiveness to maternal tonic signals. Secondly, the larger vessels, such as the uterine and radial arteries, dilate to increase the amount of blood and nutrients that are supplied to the uterus as the fetus continues to develop; the remodeling of the spiral arteries occurs as a result of the release of hormones from the placenta (James, Chamley, & Clark, 2017).

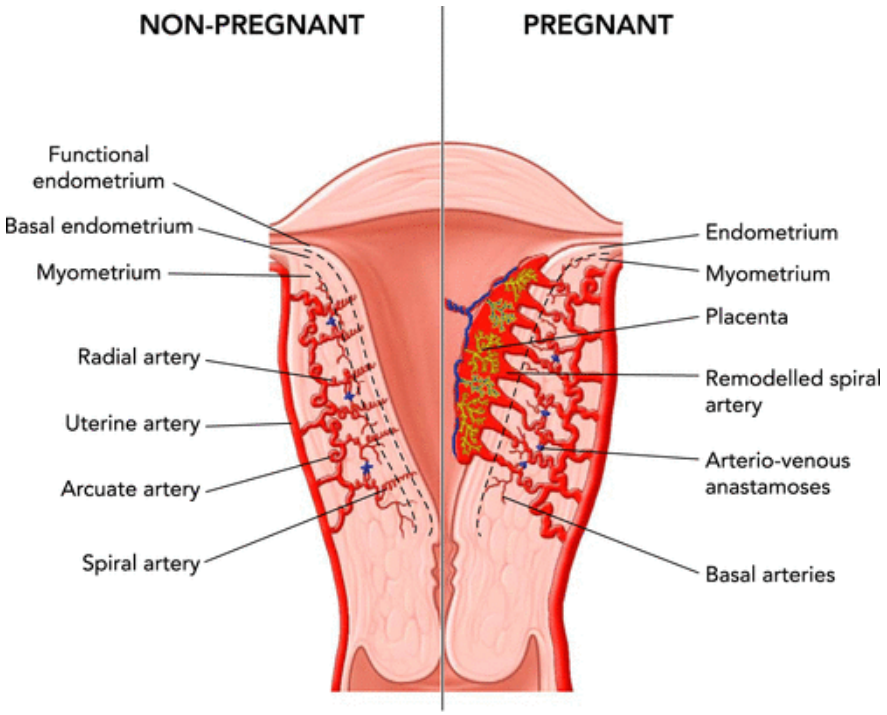

Figure 1: Anatomy of the major uterine blood vessels in the non-pregnant and pregnant uterus

3.7 Spiral Arteries Remodelling

Spiral artery remodeling is a necessary process that occurs during pregnancy. This process is initiated by the invading trophoblasts, specialized cells forming the placenta's outer layer. The trophoblasts migrate into the maternal decidua and myometrium, interacting with the maternal spiral arteries. During the first trimester of pregnancy, the trophoblasts induce apoptosis of the vascular smooth muscle cells and endothelial cells that line the spiral arteries. This leads to the loss of the muscular and elastic components of the vessel wall, resulting in the broader artery (Whitley & Cartwright, 2009).

The remodeling of the spiral arteries is essential for establishing and maintaining a healthy pregnancy. Failure of this process can lead to various pregnancy complications, such as FGR. Despite its importance, the mechanisms underlying spiral artery remodeling still need to be fully understood (Whitley & Cartwright, 2009).

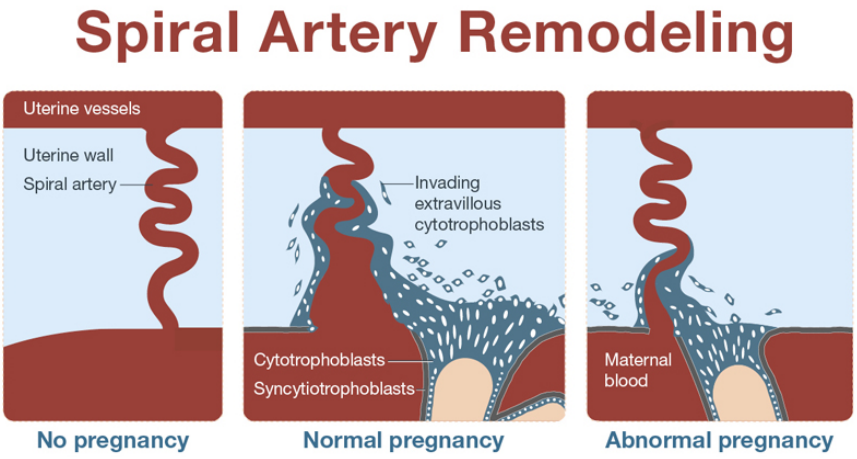

Figure 2: Showing the remodelling process on spiral arteries between a non pregnant, normal pregnant, and pathological scenario of impaired remodelling.

3.8 Arcuate and Radial artery remodelling

The uterine, arcuate, and radial arteries, situated upstream from the spiral arteries, play a critical role in regulating peak blood flow. However, the understanding of these arteries is limited. Although changes in the uterine vasculature can be observed, quantifying the extent of their remodeling is challenging due to their deep location within the uterine myometrial tissue, preventing their exit from the uterus after birth, and their small size, which makes accurate imaging difficult with most pregnancy-safe modalities such as MRI and ultrasound.

There is some quantified evidence of changes in these vessels during pregnancy. For instance, the uterine artery's lumen diameter doubles by seven weeks of gestation, and the radial artery's lumen diameter increases by 220% at term (Osol & Mandala, 2009). These changes indicate significant remodeling, but they only provide snapshots of how these changes progress throughout pregnancy. Moreover, it remains unclear how geometric parameters like vessel uncoiling and elongation respond to vessel width and uterine size increases.

3.9 Medical Imaging Analysis on Boyd Collection

Histology is concerned with various methods of examining a biological specimen at a microscopic level of a thin tissue section. Cutting through a specimen reveals its internal topography, and staining the sections allows the observation of complex differentiated structures. These histology slides can be digitalized, creating high-resolution images that can be used for image computing and machine learning algorithms, possibly allowing disease detection and different structures in that slide.

If someone would like to examine a specimen digitally in a 3D perspective, they need to process 2D digital images into a 3D form. By stacking the 2D slides on top of each other, you can recreate the structure in 3D. However, when doing this, does this method regain all the information as if the structure were in 3D? This is not to be the case due to many

factors. The slicing of the structure in 2D slides breaks the spatial relations between the 2D slides and creates discontinuities (Pichat, Iglesias, Yousry, Ourselin, & Modat, 2018).

3D histology reconstruction is a method that allows observation of otherwise invisible structures of the internal topography of a specimen. As mentioned previously, the uterus is one of the most poorly understood organs in the human body, especially during pregnancy, due to limitations such as the rapid development of the uterus and the inaccessibility of direct measurements during pregnancy, as you would not proceed with any invasive techniques that could have an impact on the developing fetus. There is a collection of uterine specimens with placenta in situ called the Boyd Collection. These specimens were prepared as tissue slides, and Jonathan Reshef was able to create 3D reconstructions from these 2D slides. During the reconstructions, Jonathan encountered many issues when aligning the 2D slides to create a 3D copy of the specimen (Reshef, 2021). When digitalizing the Boyd Collection, they first need to turn from a soft tissue into a series of thinly preserved slices stored on slides, where they are embedded in paraffin blocks where the slides can also be stained if desired to highlight the different structures in that slide.

Once the specimen is removed from the subject, there are artefacts that are introduced that can't be reversed as damage can happen to the specimen when being removed, such as cuts, compression, and tension. This will affect when recreating a 3D copy of the specimen when trying to line up the slides. Another artefact that can occur when preparing slides is that features can disappear. However, this issue can be fixed by choosing one stain to allow for minimal variations (Reshef, 2021).

3.10 ImageJ Image Analysis on Placental Histological sections

ImageJ is a public-domain software that is widely used for image analysis in various fields, including biology, medicine, and engineering. It is a versatile tool that allows users to perform various image processing and analysis tasks, such as measuring object size, shape, and intensity, counting particles, and tracking objects over time. ImageJ can handle a variety of image formats, including tiff and jpg files.

A case ImageJ was used in a study to automate image analysis of placental villi and syncytial knots. With this technology hundreds of histologic images within minutes using macro commands could be analysed, showing the efficiency and speed of automation to return data for analysis. Techniques involved include colour thresholding and edge detection to distinguish the blood vessels (Kidron, Vainer, Fisher, & Sharony, 2017). The variables used for analysis included measurements and shape descriptors of the villi and syncytial knots, such as area, perimeter, diameter, and circularity. The techniques used here could be carried out on to this project where different measurements and shape descriptors can be taken on the digitized Boyd Collection slides where uterine changes could be identified at different stages of pregnancy.

3.11 Deep Placental Vessel Segmentation in Fetoscopic Images

Fetoscopy is a procedure where a small instrument (laparoscope) is inserted into the uterus in order to see the fetus and placenta (J. H. Medicine, n.d.). A U-Net architecture convolutional neural network (CNN) is commonly used for biomedical image segmentation tasks, to segment placental vessels. The trained U-Net model is then used to segment new images by predicting a label for each pixel based on its features (Bano et al., 2020). Overall, machine learning, especially pixel-wise segmentation using the U-Net architecture, is used to solve the problem of identifying and segmenting placental vessels. The problem being faced is similar in the way that this project also is looking at placental vessels, by applying a similar approach of using pixel-wise segmentation it will allow a good method to identify different regions of the placenta.

4 Methods

4.1 Data Collection

The Boyd Collection is an archival collection of human embryonic material held at the University of Cambridge. The placental samples fall into two categories: placenta-in-situ specimens and isolated placental specimens. Few clinical details are available from which to assess the normality of the samples. (Centre for Trophoblast Research). These embryonic materials are sole histological sections, meaning that the larger tissue blocks have been cut to thin tissue slices. Due to the slicing of tissues, unwanted artefacts are introduced to the slices, which can impact any future analysis of these specimen. The moment the specimen is removed from the subject, irreversible artefacts are introduced. Unless the tissue has been imaged in vivo prior to removal, the original volume can never be recreated again. (ReshefJonathan, 2021). The sections have been scanned on a high-resolution flat-bed scanner, and both low and high-resolution files are available. The high-resolution files have been tiled using Zoomify, allowing viewers to move around the section. (Centre for Trophoblast Research). These high-resolution images were processed and used in the analysis.

Before starting with any analysis, a better understanding of the structure of these placental specimens was required. To do this a few examples of slices of placental specimens at different gestational ages were printed out and tried to label different sections of the tissues. After labeling these sections with the supervisor, the examples were gone through to make sure the labels were correct or if anything needed corrections so the theory is correct when images are analyzed later on. The images had a corresponding mask with the following labels: 255 = background, 254 = unlabelled, 1 = myometrium, 2 = decidua, villous. The masks having pixel values between 1-255, means that they could be represented as a greyscale image.

The myometrium is a thick, smooth, and muscular layer and has a pale pinkish colour and a well-defined appearance. The muscle is defined as dark red paths dense of tissue. The blood vessels are represented by empty black spaces, not that they are not the background. The decidua has a reddish or pinkish appearance with lots of circular glands, due to increased vascularity, particularly during early pregnancy. Visually, the villous appears as numerous finger-like projections or structures that extend from the fetal side of the placenta into the maternal blood-filled spaces within the uterus.

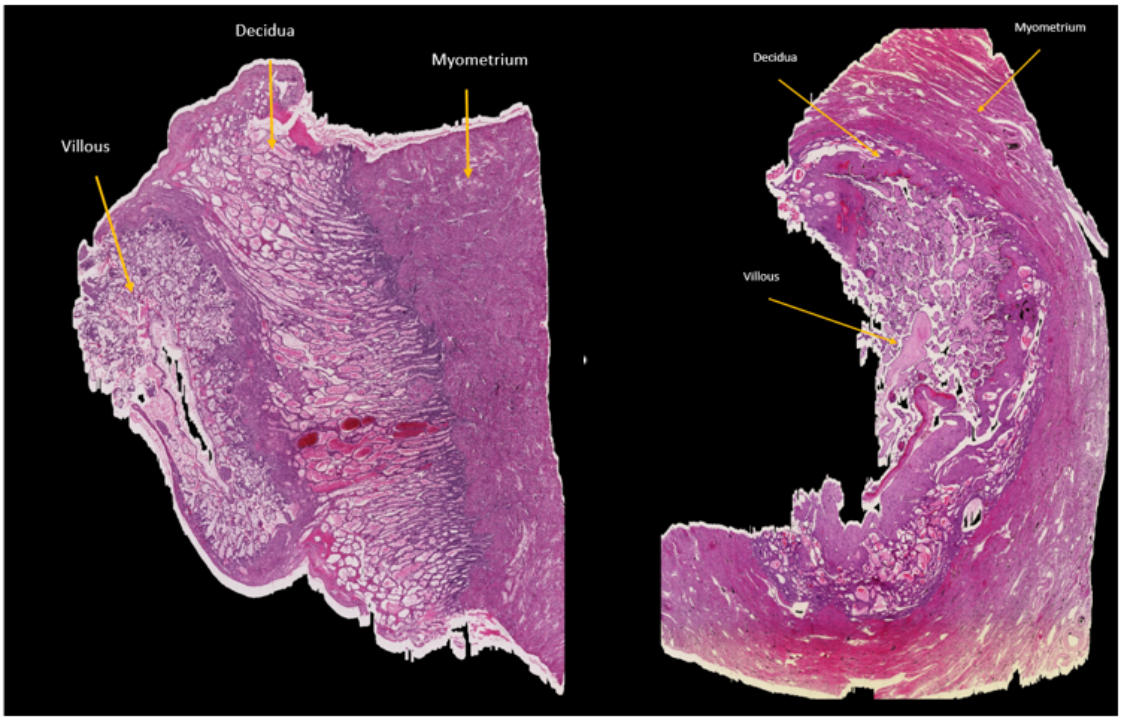

Figure 3: a: 6 weeks in b: 11 weeks in

4.2 Setting up the Environment

Initially, the project began with working with some code left by Jonathan Reshef, who worked on a 3D Virtual reconstruction of the uterus and had done some image segmentation to label some images to try and fix artefacts that were created when slicing tissue blocks into thin slices. An environment was set up using Anaconda Navigator, which allows us to create an isolated environment where specific versions of packages can be used without interacting with the existing default package versions. However, when trying to set up the environment from the 3D Histological Reconstruction repository, many errors needed to be dealt with.

The first issue that was encountered was compatibility issues with dependencies having versions that clashed with another package's version. When installing the packages required from the requirements.txt file, if a certain NumPy version existed, then the TensorFlow version that was currently installed would not be compatible with that NumPy version and require a different version in a specific range, and when the new NumPy version was satisfied, then that version would flag that the NumPy version is not compatible with a different package. This sequence of events happened multiple times but for multiple different packages. Eventually, a different approach was carried out. The approach that was taken was just the package names in the requirements file. This allowed Pip to decide package versions compatible with all others automatically and install them. This fixed the compatibility issue.

```
absl-py==1.4.0
astunparse==1.6.3
cachetools==5.3.1
certifi==2023.5.7
charset-normalizer==3.1.0
contourpy==1.0.7
cycler==0.11.0
flatbuffers==23.5.26
fonttools==4.39.4
gast==0.4.0
google-auth==2.19.0
google-auth-oauthlib==1.0.0
google-pasta==0.2.0
grpcio==1.54.2
h5py==3.8.0
idna==3.4
imageio==2.30.0
jax==0.4.10
joblib==1.3.1
keras==2.12.0
Keras-Applications==1.0.8
Keras-Preprocessing==1.1.2
kiwisolver==1.4.4
lazy_loader==0.2
libclang==16.0.0
Markdown==3.4.3
MarkupSafe==2.1.2
tensorflow==2.12.0
tensorflow-addons==0.20.0
tensorflow-intel==2.12.0
termcolor==2.3.0
tifffile==2023.4.12
typing_extensions==4.6.2
urllib3==1.26.16
wrapt==1.14.1
matplotlib==3.7.1
ml-dtypes==0.1.0
networkx==3.1
numpy==1.23.5
oauthlib==3.2.2
opencv-python==4.7.0.72
opt-einsum==3.3.0
packaging==23.1
pandas==2.0.2
Pillow==9.5.0
plotly==5.14.1
protobuf==4.23.2
pyasn1==0.5.0
pyasn1-modules==0.3.0
pyparsing==3.0.9
python-dateutil==2.8.2
pytz==2023.3
PyWavelets==1.4.1
requests==2.31.0
requests-oauthlib==1.3.1
rsa==4.9
scikit-image==0.20.0
scikit-learn==1.3.0
scipy==1.10.1
six==1.16.0
tenacity==8.2.2
tensorboard==2.12.3
tensorboard-data-server==0.7.0
tensorflow-estimator==2.12.0
tensorflow-io-gcs-filesystem==0.31.0
threadpoolctl==3.1.0
typeguard==2.13.3
tzdata==2023.3
Werkzeug==2.3.4
```

Figure 4: List of dependencies used

Another issue faced was the difficulty of running Jonathan's code due to numerous errors related to missing files. This situation likely arose from multiple individuals collaborating on the code without ensuring that other pieces of code were updated when specific files were modified. As a result of the inability to execute Jonathan's code successfully, the decision was made to initiate the project from scratch, beginning with the image segmentation documentation and proceeding from that point.

A python script was created, it would run all the terminal commands that would create the environment by creating a virtual environment that ran on Python version 3.10, installing all the dependencies via requirements.txt, and opening VS Code to start the project. This was done for convenience because on the university computers, every time a new computer had to be logged into, the terminal commands would have to run again to set up the environment.

The main dependencies used were Keras, Tensorflow, Matplotlib, Numpy, Pandas, and Sci-Kit. Keras is a high-level neural networks API that provides a user-friendly interface for building and training neural networks. TensorFlow, an open-source machine learning framework, serves as the backend for Keras, offering extensive tools and resources for developing deep learning models. Matplotlib is a versatile data visualization library used for creating plots and charts. Numpy is the fundamental package for scientific computing in Python,

offering support for arrays and matrices, making it indispensable for data manipulation and numerical operations.

4.3 Filtering out Images

The Boyd collection has a lot of slides of tissue at different gestational weeks. The folder `H653A_11.3` is the only folder currently that has manual masks created by The Development and Reproductive Health team at Auckland Bioengineering Institute, out of the 195 slides, only 15 of those slides have these manually labeled masks. The decision was made to work on just these files, so from the research drive they were copied into a private repository that will be worked on in a folder named Masks and Images. A function was also created that iterates through the images and masks folder and returns a list of paths that refers to the paths of the images and their corresponding masks.

Two different checks were made in the function. The first check was to make sure the files were a png file and that the first character of the file name is a capital H. This was done to deal with any non-png files that were in the folder, an example was the Thumbs.db file, which is a thumbnail cache file, trying to delete it from the folder will not delete it, and the capital H check is to make sure only the useable images and masks are selected. Both examples are files that are hidden, so if the code was ran without this check, errors would be encountered later.

The second check is to make sure that the images and masks list only contain images and masks where the corresponding mask have manually labelled masks, these labels will be useful when training the data giving us the ability to do supervised learning.

4.4 Splitting to Sub-Images

After filtering the images and masks, a dataset with only fifteen data points remains, which needs to be revised for training a machine learning model. To increase the dataset's size, the decision was made to divide the fifteen images and their corresponding masks into smaller sub-images. Each image and mask has dimensions of 1424 by 2006 pixels. To ensure there are no leftover pixels, the images were split where the height and width are both divisible by specific numbers, resulting in sub-images measuring 118 pixels in height and 178 pixels in width. How it was split can be seen in the figure below.

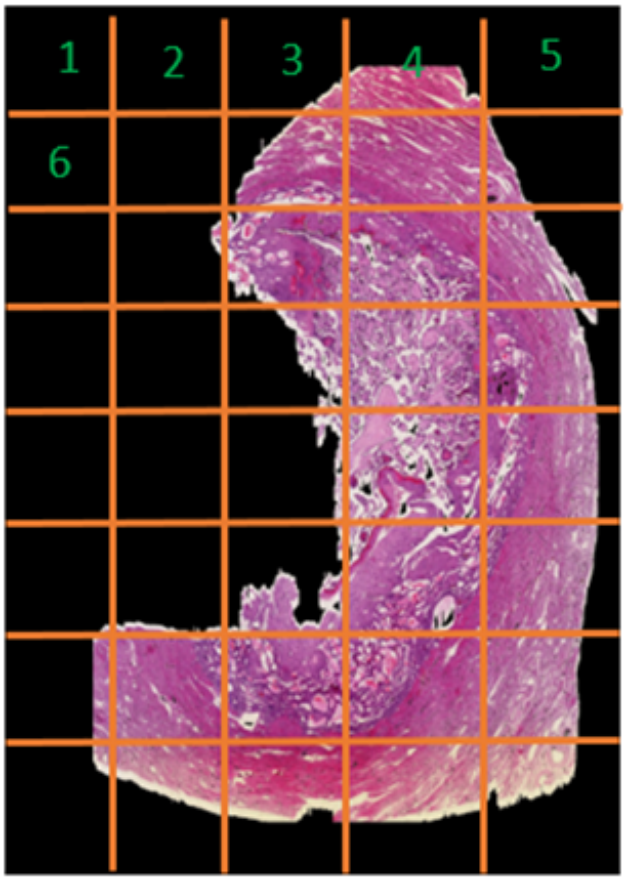

Figure 5: Method to Split Images

4.5 Decoding to Tensors

The images cannot be directly input into a machine-learning model; they need to be decoded into tensors. To accomplish this, a function was created that takes the sub-image and mask paths as input and decodes them into tensors. Tensors provide a powerful and flexible way to represent and process data in various mathematical and computational applications. For the images, they were decoded using three channels, considering that they are RGB images, with a data type of 8 bits unsigned, where values range from 0 to 255. In the case of the corresponding masks, they were decoded using one channel, resulting in a greyscale image output with a data type of 16 bits unsigned integer. It's worth noting that the necessity for 16 bits in masks, despite pixel values ranging from 0 to 255, is because of the software the images were created in. They would be able to be converted to 8-bit without a loss of information.

4.6 Verify Corresponding Pairs and Removing Unnecessary Images

For a sanity check a plot of a pair of image and mask was created to make sure that the image and mask are in the same index, by getting the same index files from the split-image

and sub-mask folders based off the index, and plotting them side by side. If there is no image and mask found, then it returns saying that there is no sub-image and mask found.

Checking a few sub images there were a few where the image was purely the background, these kinds of images provide no useful information and will not help in training the machine learning model as there is no tissue to differentiate from the background. A function was developed that checks if the image is all black, meaning it is just the background, if it is so the image and corresponding mask and its paths were removed, refer to Figure 6 below that shows an example of a corresponding image and mask.

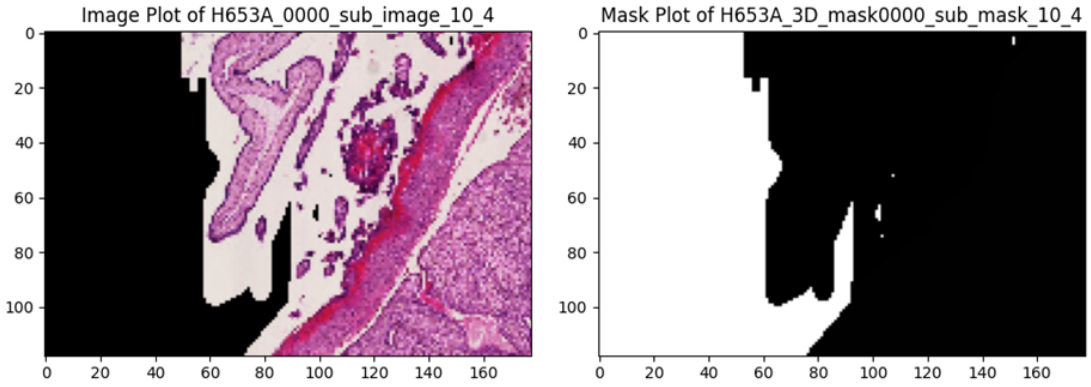

Figure 6: Example of Corresponding Image and Mask

4.7 Choice of Machine Learning Models and Tasks

There were many decisions made when deciding what kind of models to train the data on and what task the model should perform. The choice made was to make the model perform pixel-wise segmentation. As each individual pixel in the sub-image and mask are labeled, and since it is desired to predict every pixel for the predicted mask, it was decided to approach this problem with pixel-wise segmentation. With the different types of machine learning models, it was settled with a U-Net structure ML model. The U-Net architecture is a popular architecture in the field of medical image segmentation. Its defining feature is a U-shaped structure consisting of an encoder path that captures and encodes spatial information through a series of convolutional and pooling layers, followed by a symmetric decoder path that reconstructs the original image's spatial resolution through deconvolution and upsampling layers.

4.8 Development of Model

4.8.1 Format of Input Data

Looking at previous work on pixel-wise segmentation indicated that generators would be a good choice to format the data into batches to be fed into the model. However, this led to an issue that occurred when developing the model. A lot of bugs were encountered that were

difficult to debug and resolve. An example of a bug that could not be solved was the format of the batches created from the generators was incompatible with the model. Similar errors from this bug were on Stack Overflow, but the methods to solve this bug were unsuccessful in correcting the issue.

A dictionary was created and stored the split data in three different keys, train, test and validation data, and from those three keys they stored the images and masks separately.

Each sub-image is 118 pixels high and 178 pixels wide. These images will be resized to 256 by 256 pixels to feed into the model to ensure when downsampling occurs, it occurs without any issues. Each batch will have a size of 16 images, with each model having a maximum epoch of 5 and predicting five different classes, which are the background, three different layers of the placenta, and unlabelled pixels. It was decided to run for five epochs because the max epochs of five had the best trade-off between the runtime of the code and the results it produced.

4.8.2 Models Training and Optimization

The different models that were experimented and trained on were ResNet, DenseNet, VGG16, VGG19, MobileNet, NasNet and EfficientNet models. These were chosen as out of the 10s of models that were trained on these were relatively the best. The reason why different versions of ResNet or DenseNet were trained on is because it was experimented with to know if there was a difference between the same kind of models with knowing that they have different number of trainable parameters. The exact models that served as a base model for the U-Net architecture were ResNet152V2, DenseNet121, VGG16, VGG19, NASNETMobile, DenseNet201 and MobileNetV2.

Each model follows a similar structure. Each U-Net model is loaded with a pre-trained model of a certain model. Followed by the U-Net architecture of upsampling and downsampling, each model will have around 700 layers, including an output layer that predicts the five different classes and also has a learning rate of 1e-3. 700 layers may be a large number of layers, but due to the dataset size, the model will hopefully not be prone to overfitting.

Running all of these models takes hours to run, so to optimise the time of each model running, early stopping callbacks in the model. The validation loss of each epoch and if it didn't improve after a certain number of epochs, the training of the model would end, and the best weights would be restored. The patience level was experimented with to find the best trade-off between the runtime of a single model and the validation loss it returned. The patience level is how many extra epochs to run after no improvement was made in the `Val_Loss` metric before stopping the model from learning any more.

4.9 Predictions Visualization

After training the models, finding the best model and making predictions on the test set, many issues resulted when visualizing the predictions. The issue was when displaying the predictions, the colours of the different classes would vary through each prediction. Some of the predictions did not contain all of the classes, so the colours were relative to the values of the classes. The class numbers had a big difference of 1,2,3,254,255. So, for example, an image containing the background, unlabelled and the myometrium. Due to 254 and 255 being relatively close, those two classes will be shown as similar colours.

To resolve this issue, numbers were assigned from 1 to 255 to the five different classes, instead of having 1,2,3,254 and 255. The outcome was an even distribution of numbers from 1-255 based on the number of classes. By allocating these new numbers, it resolved the issue of different classes appearing in the same colour. Matplotlib's default colour map is Viridis. Even if a considerable value separates the values, the viridis colour allows those differences to be perceived as roughly constant, giving the ability to distinguish the different tissue regions.

4.10 Python Image Analysis

Initially, image analysis was going to be done through the tool ImageJ, however with the lack of expertise and experience with this image processing program, it was decided to use Python, focusing on the package sci-kit-image, an open-source library that contains a wide range of collection of algorithms for image processing.

Edge detection was commonly used in similar projects to extract the vessels and glands from the tissue. Initially, frequently used edge detection filters such as canny edge detection and Sobel filters were tested, but the desired results of identifying the vessels and glands still needed to be achieved.

In the end, a Gaussian blur was applied to the original image to enhance object boundaries and reduce any noise. The blurred image is then converted to greyscale, and a threshold is used to create a binary mask, where pixels above the threshold are considered part of the objects of interest. Small noise (regions that contained a few pixels) that weren't part of any region of interest were removed based on the region size. Then, using the OpenCV package, contours were drawn to outline the regions of interest.

5 Results and Discussion

5.1 Machine Learning Model Results

The ResNet152V2 model achieved an accuracy of 0.900, with a training loss of 0.255 and a validation loss of 0.232. DenseNet121 showed an accuracy of 0.909, accompanied by a training loss of 0.240 and a validation loss of 0.218. VGG16 gave an accuracy of 0.928, with a training loss of 0.265 and a validation loss of 0.245. VGG19, on the other hand, achieved an accuracy of 0.890, with a training loss of 0.255 and a validation loss of 0.230. The NASNetMobile model yielded an accuracy of 0.908, with a training loss of 0.270 and a validation loss of 0.285. The MobileNetV2 achieved an accuracy of 0.917, with a training loss of 0.247 and a validation loss of 0.265 and finally the results for the DenseNet201 model will be presented later.

Out of the different patient levels that was experimented with, the best performing patient level was a patient level of four, identifying the best model was harder to determine. Initially the optimum model was chosen through the metric `train_loss`, this led to VGG19 being the favourable model, however with more reasoning it was identified that the metric used to choose the optimal model should be `val_loss` as the best model should be leading in predicting on unseen data, which was the DenseNet201 model. The model had an accuracy of 0.9115, a loss of 0.2398 and a validation loss of 0.2150, even with a low learning rate of 0.001 the model loss function plateaued very quickly.

A great thing the model does is have the ability to predict the general area of the different regions of the placental tissue. It does not predict each region perfectly, however this model was only trained on 5 epochs, with more epochs it could potentially predict the general area of each region, however an issue the model constantly had was that while it was able to identify the black background of the tissue images, it was having a hard time identifying the areas of background that were visible in between the gaps of the tissue, which led to the wrong class being predicted in that area.

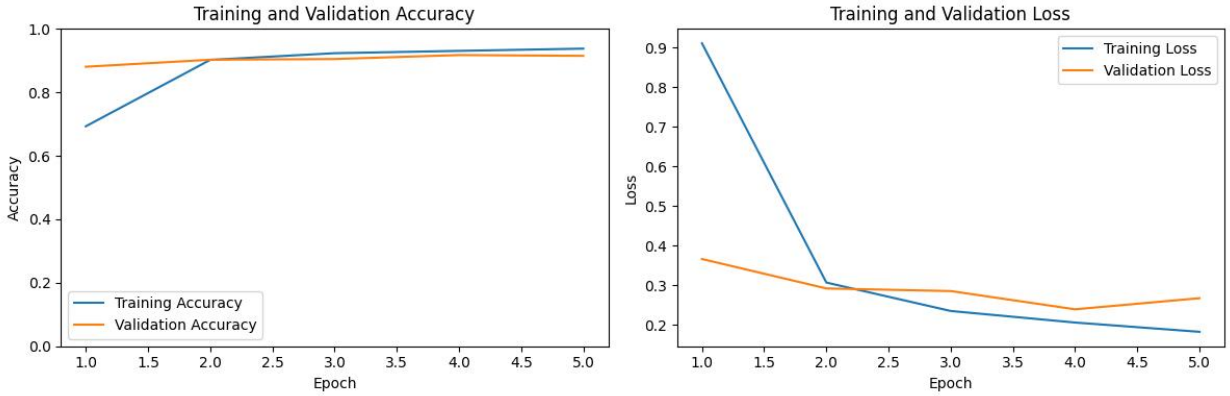

Figure 7: Accuracy and Loss of DenseNet201 Model

There were many shortcomings with this model despite it being the best, the model consistently was not able to predict the black background gaps and it wasn't able to perfectly

predict the regions of the tissue. What could be done to tackle these problems? The model could be trained on a higher number of `MAX_EPOCHS` to see if the model is able to predict better on unseen data. Something to be careful with increasing the number of epochs is to not train the model so that it is overfitting and just learning the patterns of the training dataset it can see. With the increase in `MAX_EPOCHS` the patience level for early stopping could be experimented with too, to see if this value needs to be adjusted.

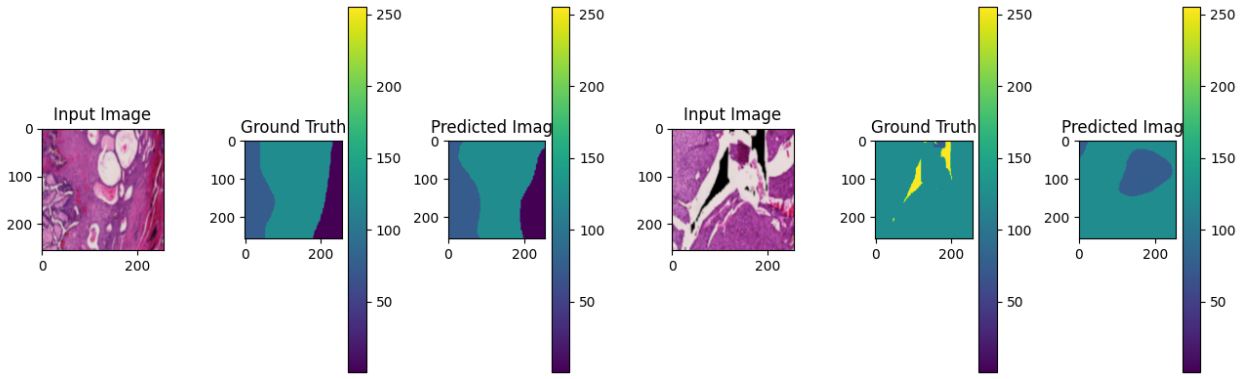

(a) Prediction with Multiple Different Regions (b) Prediction with Black Background In Gaps

Figure 8: Two Different Predictions

5.2 Python Image Analysis Results

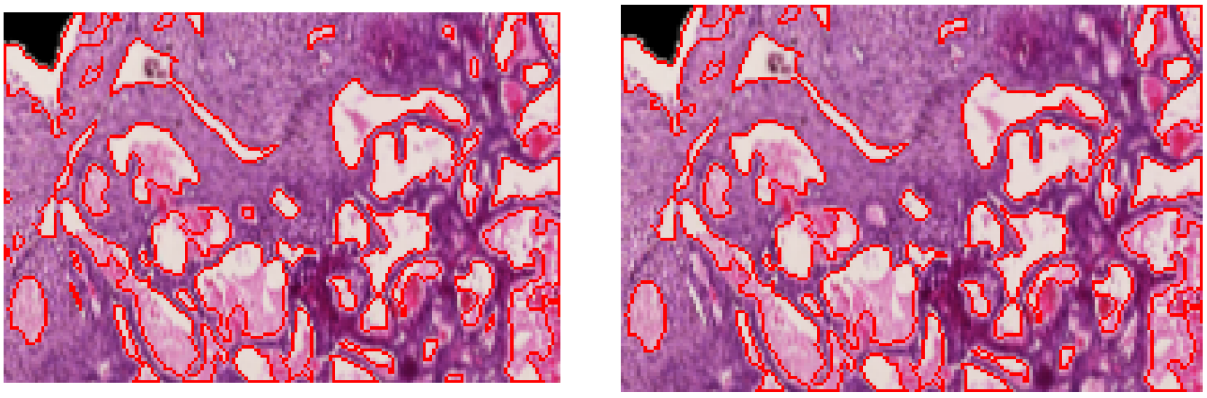

(a) Weak Noise Remover (b) Aggressive Noise Remover

Figure 9: Gaussian Edge Detection

Adjusting the threshhold values changes how much of a certain feature will be counted as a region of interest, while the `min_region_size parameter` impacts how much of the unwanted noise is removed. What this technique did well was capture most of the glands

and blood vessels, refer to the figure above. A lot of the blood in the glands and vessels were pink, what the algorithm couldn't do was capture the bright red vessels and didn't consider them a region of interest. What could be done is perhaps apply a filter to make the dark red pixels to appear more of a lighter pink colour but make sure it is easily differentiable from the rest of the tissue that is a red/purple colour.

5.3 Combining the Results

With a ML model that is able to predict different regions of placental tissue, and an algorithm that can detect different glands and vessels from placental tissue. This information that is available will allow users to identitfy the different uterine arteries, based on the shape and size of the arteries from the algorithm and also based on what region of the placental tissue it is from using the ML model.

6 Conclusion

The aim of this project was to investigate the vascular adaptation to pregnancy, focusing on the changes in blood flow and vessel structure during pregnancy to monitor any symptoms of potential FGR. Feature extraction was identified as a key image processing procedure to enable the derivation of meaningful information that can be used to understand the physiological changes that occur in the mother's body to support the developing fetus, another technique identified was pixel-wise segmentation to identify different regions of placental tissue.

The focus of this report was the implementation of a machine learning model to segment and extract different regions of the placenta, a U-Net architecture neural network model based on the DenseNet201 model was implemented to achieve this objective. Another focus was the algorithm to identify placental blood vessels and glands. By applying a Gaussian filter and other image manipulation techniques the technique can easily identify blood vessels and glands.

Overall, this report provides a valuable contribution to the understanding of vascular remodelling in pregnancy, and will help towards the understanding of uterine changes during pregnancy. This project can serve as a foundation of possibly integrating these two techniques and implementing a machine learning model that can identify the glands and blood vessels along side which region of placental tissue they reside in.

References

Allerkamp, H. H., Pole, T., Boukham, A., James, J. L., & Clark, A. R. (2022). Pregnancy-specific uterine vascular reactivity: a data-driven computational model of shear-dependent, myogenic, and mechanical radial artery features. *American Journal of Physiology-Heart and Circulatory Physiology*, *323*(1), H72-H88. Retrieved from https://doi.org/10.1152/ajpheart.00693.2021 (PMID: 35452318) doi: 10.1152/ajpheart.00693.2021

Ameer, M. A., Fagan, S. E., Sosa-Stanley, J. N., & Peterson, D. C. (2022). Anatomy, abdomen and pelvis: Uterus. In *Statpearls.* StatPearls Publishing.

Bano, S., et al. (2020). Deep placental vessel segmentation for fetoscopic mosaicking. In *Medical image computing and computer assisted intervention – miccai 2020* (Vol. 12263). Cham: Springer. doi: 10.1007/978-3-030-59716-0_73

Clinic, C. (2022). *Human chorionic gonadotropin* (Tech. Rep.). Retrieved from https://my.clevelandclinic.org/health/articles/22489-human-chorionic-gonadotropin

Gasner, A., & P A, A. (2023). Physiology, uterus. In *Statpearls.* StatPearls Publishing.

Gude, N. M., Roberts, C. T., Kalionis, B., & King, R. G. (2004). Growth and function of the normal human placenta. *Thrombosis Research*, *114*(5-6), 397–407. doi: 10.1016/j.thromres.2004.06.038

James, J. L., Chamley, L. W., & Clark, A. R. (2017). Feeding your baby in utero: How the uteroplacental circulation impacts pregnancy. *Physiology*. Retrieved from https://journals.physiology.org/doi/full/10.1152/physiol.00033.2016 doi: https://doi.org/10.1152/physiol.00033.2016

Kidron, D., Vainer, I., Fisher, Y., & Sharony, R. (2017). Automated image analysis of placental villi and syncytial knots in histological sections. *Placenta*, *53*, 113-118. Retrieved from https://www.sciencedirect.com/science/article/pii/S0143400417302266 doi: https://doi.org/10.1016/j.placenta.2017.04.004

Madendag, I. C., Sahin, M. E., Madendag, Y., Sahin, E., Demir, M. B., Acmaz, B., ... Muderris, I. I. (2019). The effect of iron deficiency anemia early in the third trimester on small for gestational age and birth weight: A retrospective cohort study on iron deficiency anemia and fetal weight. *BioMed research international*, *2019*, 7613868. doi: 10.1155/2019/7613868

Medicine, J. H. (n.d.). *Fetoscopic laser surgery* (Tech. Rep.). Retrieved from \url{https://www.hopkinsmedicine.org/gynecology-obstetrics/specialty-areas/fetal-therapy/fetal-interventions-procedures/fetoscopic-laser-surgery}

Medicine, S. (n.d.). *Fetal growth restriction* (Tech. Rep.). Retrieved from https://discord.com/channels/844018117393907772/844018118758367234/1161126559801933924

Morley, L., Debant, M., Walker, J., Beech, D., & Simpson, N. (2021, Sep 15). Placental blood flow sensing and regulation in fetal growth restriction. *Placenta*, *113*, 23-28. Retrieved from https://doi.org/10.1016/j.placenta.2021.01.007 doi: 10.1016/j.placenta.2021.01.007

Nardozza, L. M., Caetano, A. C., Zamarian, A. C., Mazzola, J. B., Silva, C. A. P., Marçal,

V. M., ... Araujo Júnior, E. (2017). Fetal growth restriction: current knowledge. *Archives of Gynecology and Obstetrics*, *295*(5), 1061–1077. Retrieved from https://doi.org/10.1007/s00404-017-4341-9 doi: 10.1007/s00404-017-4341-9

NCT. (2018). *Pregnancy hormones* (Tech. Rep.). Retrieved from https://www.nct.org.uk/pregnancy/how-you-might-be-feeling/pregnancy-hormones-progesterone-oestrogen-and-mood-swings

Osol, G., & Mandala, M. (2009). Maternal uterine vascular remodeling during pregnancy. *Physiology (Bethesda, Md.)*, *24*, 58–71. doi: 10.1152/physiol.00033.2008

Pichat, J., Iglesias, J. E., Yousry, T., Ourselin, S., & Modat, M. (2018). A survey of methods for 3d histology reconstruction. *Medical image analysis*, *46*, 73–105. doi: 10.1016/j.media.2018.02.004

Reshef, J. (2021). *3d virtual reconstruction of the uterus* (Unpublished master's thesis). University of Auckland, Auckland.

Sapehia, D., Thakur, S., Rahat, B., Mahajan, A., Singh, P., & Kaur, J. (2021). Chapter 7 - epigenetic regulation during placentation. In T. Tollefsbol (Ed.), *Epigenetics and reproductive health* (Vol. 21, p. 117-152). Academic Press. Retrieved from https://www.sciencedirect.com/science/article/pii/B9780128197530000076 doi: https://doi.org/10.1016/B978-0-12-819753-0.00007-6

Sun, C., Groom, K. M., Oyston, C., Chamley, L. W., Clark, A. R., & James, J. L. (2020). The placenta in fetal growth restriction: What is going wrong? *Placenta*, *96*, 10-18. Retrieved from https://www.sciencedirect.com/science/article/pii/S0143400420301363 doi: https://doi.org/10.1016/j.placenta.2020.05.003

Thornburg, K. L., Jacobson, S.-L., Giraud, G. D., & Morton, M. J. (2000). Hemodynamic changes in pregnancy. *Seminars in Perinatology*, *24*(1), 11-14. Retrieved from https://www.sciencedirect.com/science/article/pii/S0146000500800476%7D (Endothelium, Derived Vasoactive Substances, and Free Radicals in Perinatal Biology) doi: https://doi.org/10.1016/S0146-0005(00)80047-6%7D

Whitley, G. S., & Cartwright, J. E. (2009). Trophoblast-mediated spiral artery remodelling: A role for apoptosis. *Journal of Anatomy*, *215*(1), 21–26. Retrieved from https://doi.org/10.1111/j.1469-7580.2008.01039.x doi: 10.1111/j.1469-7580.2008.01039.x